IEEE Access
Multidisciplinary | Rapid Review | Open Access Journal

Received June 30, 2020, accepted July 16, 2020, date of publication July 23, 2020, date of current version August 5, 2020.

Digital Object Identifier 10.1109/ACCESS.2020.3011421

Joint Optimization Method of Airborne MIMO Radar Track and Radiated Power Based on Mutual Information

XIANGYU FAN[1,2], PENG BAI[1,2], HONGWEI WANG[3], JIAQIANG ZHANG[1,2], AND HUANYU LI[1,2]

[1]Air Traffic Control and Navigation College, Air Force Engineering University, Xi'an 710051, China
[2]Shaanxi Province Laboratory of Metasynthesis for Electronic and Information System, Air Force Engineering University, Xi'an 710051, China
[3]College of Aeronautical Engineering, Air Force Engineering University, Xi'an 710051, China

Corresponding author: Huanyu Li (huanyu_li_afeu@sina.com)

This work was supported in part by the National Natural Science Foundation of China (NSFC) under Grant 61871397 and Grant 61501505; and in part by the Natural Science Foundation of Shaanxi Province under Grant 2017JQ6035.

ABSTRACT The mutual information (MI) is used as the target function to jointly optimize the space trajectory and radiated power of the airborne MIMO radar. By adjusting the space position of the radar and radiating energy in real time, the detection efficiency of the MIMO radar is improved. Firstly, the cooperative detection model of aviation swarm MIMO radar is constructed to quantitatively describe the relationship between radar position and radiated power parameters and echo. Therefore, the MI between the transmitted signal and the received signal at the same time is derived, and the MI of the radar echo at the current time and the next time is derived. Maximizing the amount of MI sent and received signals can improve the amount of information detected, and minimizing the amount of MI at adjacent moments can improve the quality of information. This paper designs a time-sharing optimization algorithm, and improves the Artificial Bee Colony algorithm (ABC) to optimize the above two MI to achieve real-time adjustment of radar position and power. Through simulation verification and algorithm comparison, the advantages of this algorithm are reflected.

INDEX TERMS Mutual information, airborne MIMO radar, space trajectory, radiated power, artificial bee colony algorithm.

I. INTRODUCTION

Multiple Input Multiple Output (MIMO) radar refers to radar systems which use multiple antennas for transmitting independent waveforms and multiple receivers for receiving target echoes [1]–[6]. Using this feature, the radar system can significantly improve the target detection, tracking, identification and parameter estimation capabilities, and achieve a good perception of the air situation.

In order to further improve the detection performance of MIMO radar, scholars have conducted intensive research. The algorithm performance of beamforming technology [7], [8] and space-time adaptive algorithm [9], [10] has been improved, and the detection capability of MIMO has been improved from the signal processing level. At the same time, scholars use or design certain criteria to improve radar detection accuracy by adjusting the parameters of radar radiated power, polarization mode and signal bandwidth, or jointly adjusting multi-dimensional parameters. Reference [11] established the relationship between MIMO radar transmitter power and Cramer-Rao lower bound (CRLB) to achieve localization minimum estimation mean-square error (MSE). The methods of minimizing radiated power for a given MSE and the method of minimizing MSE at a given power are studied separately. Reference [12] uses CRLB as the optimization objective function to realize the optimization of radar scheduling and radiated power of MIMO radar. Reference [13] through the optimization of power and time width, the total posterior Cramer-Rao lower bound (PCRLB) of all targets is minimized. Reference [14] uses CRLB as an evaluation index to achieve joint optimization of radiated power and signal bandwidth, to achieve more accurate detection of multiple targets. Reference [15]

The associate editor coordinating the review of this manuscript and approving it for publication was Wei-Chang Yeh.

on this basis, deduced the predicted PCRLB in the worst. The modified particle swarm optimization is used to optimize the power and bandwidth allocation strategy, which makes the detection efficiency closer to PCRLB. Reference [16] derived the Bayesian CRLB for multi-target tracking based on the Bayesian information matrix. Using this as an indicator, a joint beam selection and power allocation (JBSPA) strategy was constructed. Reference [17] proposed a distributed fusion architecture that uses covariance intersection (CI) fusion to reduce the uncertainty of system information, and derives the Bayesian CRB under this architecture. Realize joint beam and power scheduling (JBPS) through optimization. In reference [18], the measurement error was used as the optimization goal, and a joint optimization method of antenna subset selection and optimal power allocation was constructed to improve the positioning accuracy of the target. Reference [19] used the prior knowledge predicted from the tracking recursion cycle to construct the relationship between radiated power and the Bayesian CRLB. By optimizing power distribution, the ability to recognize multiple targets in a clutter environment is improved. Reference [20] combines priority statistic information of targets to construct the optimality condition decomposition (OCD)-based and the alternating direction method of multipliers based algorithms. Based on that, a strategy for minimizing radiated power under a given MSE is derived. Reference [21] based on game theory, by optimizing the radiated power, improved the signal-to-interference-plus-noise ratio (SINR) under Nash equilibrium conditions. Reference [22] studied separately in the context of a strategic non-cooperative game and Stackelberg game, by optimizing beamforming and resource allocation, to meet the detection needs. Reference [23] considers radar and jamming as a two-player zero-sum (TPZS) game. By adjusting the polarization mode of the radar signal, the SINR of the radar is improved, and the purpose of weakening the interference effect is achieved. Reference [24] constructed a robust chance constrained power allocation (RCC-PA) method according to the target radar cross section (RCS) fluctuation model under different conditions to achieve the required detection accuracy with minimized multi-beam radiation power. Reference [25] derived the predicted conditional CRLB (PC-CRLB) in a cluttered environment, and designed a closed-loop feedback scheme, through joint subarray selection and power allocation (JSSPA) strategy to achieve the best PC-CRLB. Reference [26] under the condition of peak-to-average ratio (PAR) constraint, through joint optimization of transmit waveform and receive filter. The SINR and integrated sidelobe level of the receiving end are improved, thereby improving the detection capability. References [27] and [28] based on information theory, by constructing the Bayesian Fisher information matrix generated by radar sequential filtering and collaborative detection, and using the Shapley value in the cooperative game to optimize it, to achieve the combination of the spatial position of the radar and the radiation strategy optimization. References [29] and [30] used compressed sensing methods to design radar waveforms and adjust radiated power, respectively to optimize the coherence between the target returns from different search cells, and minimize the coherence value of the sensing matrix, improving radar detection efficacy. References [30] and [31] studied the optimization of the radiation strategy that can achieve the target detection requirements under low interception requirements. While reducing the possibility of signal interception, it also reduces the energy consumption of the system.

The above-mentioned literature improves the detection efficiency of radar by adjusting parameters such as radar radiation strategy and signal bandwidth. The performance of MIMO radar is closely related to the spatial configuration of the receiver [33]. At the same time, with the development and maturity of MIMO radar technology, the realization of airborne MIMO radar is an important trend of future radar development [34]–[37]. The obvious advantage of airborne MIMO radar compared to ground MIMO is that it can adjust the position to achieve better detection, that is, improve the detection performance by optimizing the spatial position. The radar can improve the detection capability through a more flexible spatial structure. But there are two important premises for this performance improvement. One is that the airborne MIMO radar is affected by kinematic constraints. The position adjustment of the MIMO radar must be based on the kinematic model of the aircraft, and the position of the MIMO radar must be continuously changing, and no jumps in position can occur. Another requirement is higher requirements for real-time performance. The computing resources carried by the aircraft itself are very limited. During the detection process of the airborne MIMO radar, it is necessary to not only process the MIMO radar signal, but also optimize the scheduling strategy of the airborne detection resources. This also has a strong demand for the real-time nature of the algorithm.

Therefore, this paper takes the airborne MIMO radar as the research object, and improves the detection efficiency of the radar by jointly optimizing the aircraft track and radiated power. From the perspective of information theory, this article regards improving radar detection capability as a problem to obtain more information about the target. Using the theory of mutual information (MI), the MI between the transmitted signal and the received signal is maximized, thereby increasing the amount of information for acquiring target information. At the same time, the MI of the echo signal at the adjacent time is minimized to reduce the amount of repeated and useless information. The optimization process of simultaneous and time-sharing is designed. Qualitative analysis and simulation verify that time-sharing optimization is more effective. The problem to be solved is converted into a continuous time series optimization problem. Using the Artificial Bee Colony algorithm (ABC) algorithm, combined with the characteristics of the algorithm and the biological characteristics of the bee to improve it, it realizes the optimization of the collaborative optimization of MIMO radar detection resources.

The remainder of this paper is organized as follows. Construct a collaborative detection model in Section II. Derive the MI of different signals in Section III. Design the optimization objective function and analyze it in Section IV. Improve the ABC (IABC) algorithm in Section V. The optimization process of MIMO radar detection resources based on IABC algorithm is designed in Section VI, simulation verification and algorithm comparison in Section VII. Conclusion is drawn in Section VIII.

II. MATHEMATICAL MODEL OF COOPERATIVE DETECTION FOR AIRBORNE MIMO RADAR

In the cooperative detection of aviation clusters, the optimal configuration of the spatial position and radiated power of each node can improve the detection efficiency to a greater extent, so as to more accurately perceive the battlefield situation in a complex dynamic environment. How to achieve rapid node configuration and radiation control is the core factor restricting the performance improvement of airborne MIMO radar.

Suppose that there are M aircraft carrying MIMO radar to coordinate detection of U targets. The signals emitted by the radar are orthogonal to each other. Suppose at time t, the coordinate of the m-th aircraft is $\mathbf{P}_{pm}^t = \left[x_{pm}^t, y_{pm}^t\right]^T$, the speed is $\mathbf{v}_{pm}^t = \left[v_{xpm}^t, v_{ypm}^t\right]^T$, $m = 1, 2, \ldots, M$. Then the position and speed of our aircraft can be expressed as $\mathbf{P}_p^t = \left[\mathbf{P}_{p1}^t, \mathbf{P}_{p2}^t, \ldots, \mathbf{P}_{pM}^t\right]$ and $\mathbf{v}_p^t = \left[\mathbf{v}_{p1}^t, \mathbf{v}_{p2}^t, \ldots, \mathbf{v}_{pM}^t\right]$. Suppose the coordinate of the u-th target is $\mathbf{T}_u^t = \left[x_{Tu}^t, y_{Tu}^t\right]^T$, the speed is $\mathbf{v}_{Tu}^t = \left[v_{xTu}^t, v_{yTu}^t\right]^T$, $u = 1, 2, \ldots, U$. The corresponding position and speed can be expressed as $\mathbf{T}_U^t = \left[\mathbf{T}_{T1}^t, \mathbf{T}_{T2}^t, \ldots, \mathbf{T}_{TU}^t\right]$ and $\mathbf{v}_U^t = \left[\mathbf{v}_{T1}^t, \mathbf{v}_{T2}^t, \ldots, \mathbf{v}_{TU}^t\right]$. In order to show clarity, the transmission and reception are divided into two figures. The schematic diagram of MIMO radar detection of multiple targets is shown in the figure below:

As can be seen from Figure 1, under the framework of MIMO radar, the detection signal transmitted by each aircraft can detect each aircraft of the other party, and the corresponding echo signal can be received by any of our aircraft. As a result, signal-level information interaction is achieved. Compared with traditional airborne radar, the detection range is wider and the situation awareness is more accurate.

To further study the system status, the i-th aircraft was selected to transmit signals to detect the u-th aircraft, and the echoes received by the j-th aircraft were analyzed. The specific state is shown in Figure 2.

According to the distance formula, the distance d_{iu}^t between the i-th transmitter and the u-th aircraft is:

$$d_{iu}^t = \sqrt{\left(x_{pi}^t - x_{Tu}^t\right)^2 + \left(y_{pi}^t - y_{Tu}^t\right)^2} \tag{1}$$

Similarly, the distance d_{uj}^t between the u-th aircraft and the j-th receiver can be calculated. Then the corresponding signal

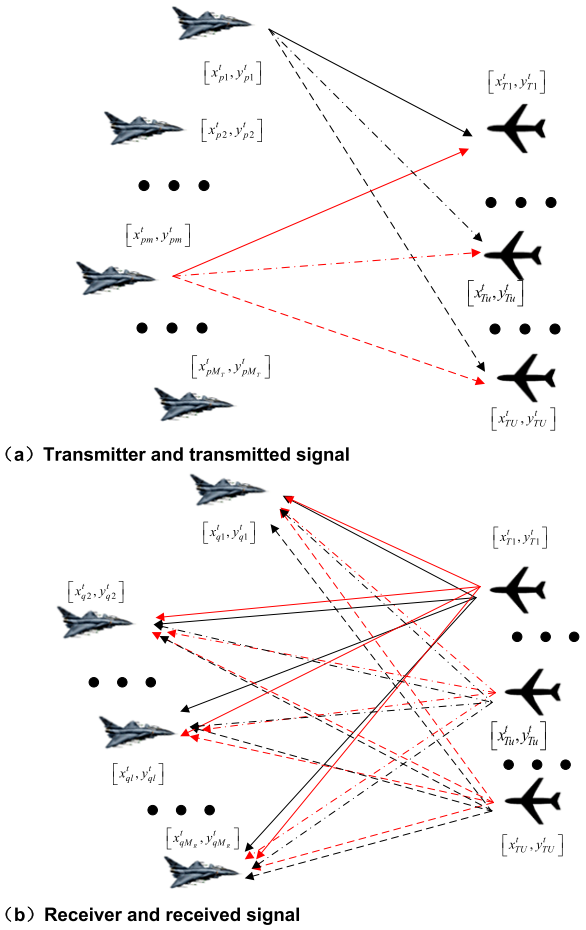

FIGURE 1. Schematic diagram of MIMO radar detecting multiple targets.

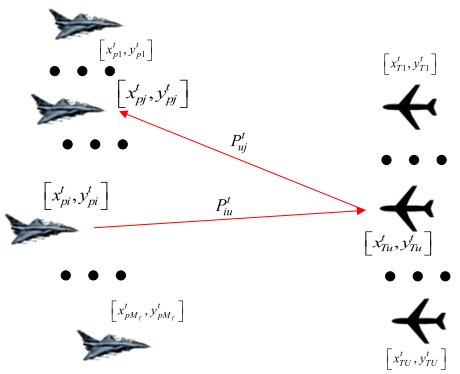

FIGURE 2. Schematic diagram of MIMO radar detection.

delay τ_{uj}^t is:

$$\tau_{ij}^t = \frac{d_{iu}^t + d_{uj}^t}{c} \tag{2}$$

where c is the speed of light, it is assumed that the detection power of all aircrafts has a power upper limit P_0. At time t, the energy of the i-th aircraft detecting the u-th aircraft is P_{iu}^t,

then it should satisfy:

$$\sum_{u=1}^{U} P_{iu}^{t} < P_0 \tag{3}$$

That is, the total energy used for detection cannot exceed the upper limit of its own power P_0. Then the echo power P_{uj}^{t} received by the j-th receiver is:

$$P_{uj}^{t} = Q_R \frac{P_{iu}^{t} G_{iu}^{t} G_{uj}^{t} \sigma_{ij}^{t}}{\left(4\pi d_{iu}^{t} d_{uj}^{t}\right)^2} \tag{4}$$

where G_{iu}^{t} is the antenna gain of the transmitter in the iu direction, G_{uj}^{t} for the same reason. σ_{ij}^{t} is the radar cross-sectional area of the target. Q_R is a substitute for system loss and space attenuation, etc. We won't introduce too much about it here. For internal specific parameters and meanings, we can refer to the radar manual. This article will treat it as a constant later. Then the signal y_{ij}^{t} received by the j-th receiver can be expressed as:

$$y_{ij}^{t}(t) = \sqrt{P_{uj}^{t}} s_{ij}^{t}\left(t - \tau_{ij}^{t}\right) + n_{ij}^{t} \tag{5}$$

s_{ij}^{t} is the transmitted signal of the radar, and n_{ij}^{t} is the white noise of the Gaussian distribution received by the receiver. Then the signal received by the j-th receiver can be expressed as:

$$\mathbf{y}_j^{t} = \sum_{i=1}^{M} h_{ij}^{t} \mathbf{x}_{ij}^{t} + n_{ij}^{t} \tag{6}$$

where $\mathbf{y}_j^{t} \in C^{K\times 1}$, C represents the complex domain. $K = K_\tau + K_s$. K_τ represents the column to be filled with 0 due to delay, and K_s is the length of the signal, where h_{ij}^{t} is,

$$h_{ij}^{t} = \sqrt{P_{uj}^{t}} = \frac{\sqrt{Q_R P_{iu}^{t} G_{iu}^{t} G_{uj}^{t} \sigma_{ij}^{t}}}{4\pi d_{iu}^{t} d_{uj}^{t}} \tag{7}$$

The signal received by the airborne MIMO radar system for multi-target detection can be expressed as:

$$\mathbf{Y} = \mathbf{X}\mathbf{H} + \mathbf{W} \tag{8}$$

where $\mathbf{Y}=[\mathbf{y}_1, \mathbf{y}_2, \ldots, \mathbf{y}_M] \in C^{K\times M}$ and $\mathbf{X}=[\mathbf{x}_1, \mathbf{x}_2, \ldots, x_M] \in C^{K\times M}$ represent the received and transmitted signal matrix of M radars. $\mathbf{H} = \left[h_{ij}\right]_{M\times M} \in C^{M\times M}$ is the system response matrix. $\mathbf{W} \in C^{K\times M}$ is the noise received by the system.

Through the above derivation and discussion, the relationship between the signals received and sent at time t of the MIMO radar system can be constructed.

III. OPTIMIZATION OBJECTIVE FUNCTION BASED ON MI

When using information theory to design radar waveforms, scholars found that the greater the MI between the radar echo and the original signal, the stronger the radar's ability to estimate and describe the target parameters. The smaller the MI of the echoes at two adjacent moments, the more information about the target will be obtained. Therefore, this section uses the results derived from the previous section to construct the MI of the radar echo and the transmitted signal at time t, and the MI of the radar echo at time t and $t+1$, respectively. Construct the corresponding optimization objective function.

A. MI BETWEEN THE TRANSMITTER AND THE RECEIVER

Calculate the MI between the transmitted signal and the received signal at time t. According to the definition of MI, the MI is obtained as follows:

$$\begin{aligned} I\left(\mathbf{Y}_t; \mathbf{H}_t | \mathbf{X}_t\right) &= h\left(\mathbf{Y}_t | \mathbf{X}_t\right) - h\left(\mathbf{Y}_t | \mathbf{H}_t; \mathbf{X}_t\right) \\ &= h\left(\mathbf{Y}_t | \mathbf{X}_t\right) - h\left(\mathbf{W}\right) \end{aligned} \tag{9}$$

where $I(\mathbf{Y}_t; \mathbf{H}_t | \mathbf{X}_t)$ represents the amount of information between the transmitter and the receiver. $h(\mathbf{Y}_t | \mathbf{X}_t)$ is the conditional entropy, which refers to the amount of information transmitted by the transmitting end to the receiving end during the process of transmitting the $\mathbf{X}_t$ signal and receiving the $\mathbf{Y}_t$ at the receiving end. It can be expressed as:

$$h\left(\mathbf{Y}_t | \mathbf{X}_t\right) = \int -p\left(\mathbf{Y}_t | \mathbf{X}_t\right) \ln\left[p\left(\mathbf{Y}_t | \mathbf{X}_t\right)\right] d\mathbf{Y}_t \tag{10}$$

where $p(\mathbf{Y}_t | \mathbf{X}_t)$ represents the conditional probability density function that $\mathbf{Y}_t$ is subject to under $\mathbf{X}_t$ conditions, which can be expressed as:

$$\begin{aligned} p\left(\mathbf{Y}_t | \mathbf{X}_t\right) &= \prod_{m=1}^{M} p\left(\mathbf{y}_{mt} | \mathbf{X}_t\right) \\ &= \prod_{m=1}^{M} \frac{1}{\pi^K \det\left(\mathbf{X}_t^H \mathbf{R}_{\mathbf{H}_t} \mathbf{X}_t + \mathbf{R}_{\mathbf{W_t}}\right)} \\ &\quad \times \exp\left[-\mathbf{y}_{mt}^H \left(\mathbf{X}_t^H \mathbf{R}_{\mathbf{H}_t} \mathbf{X}_t + \mathbf{R}_{\mathbf{W_t}}\right)^{-1} \mathbf{y}_{mt}\right] \\ &= \frac{1}{\pi^{MK}\left[\det\left(\mathbf{X}_t^H \mathbf{R}_{\mathbf{H}_t} \mathbf{X}_t + \mathbf{R}_{\mathbf{W_t}}\right)\right]^M} \\ &\quad \times \exp\left\{-\mathrm{tr}\left[\mathbf{X}_t^H \mathbf{R}_{\mathbf{H}_t} \mathbf{X}_t + \mathbf{R}_{\mathbf{W_t}}\right]^{-1} \mathbf{Y}_t^H \mathbf{Y}_t\right\} \end{aligned} \tag{11}$$

where $\mathbf{R}_{\mathbf{H}_t}$ and $\mathbf{R}_{\mathbf{W_t}}$ represent the covariance matrix of $\mathbf{H}_t$ and $\mathbf{W}_t$, respectively:

$$\begin{cases} \mathbf{R}_{\mathbf{H}_t} = E\left\{\mathbf{H}_t^H \mathbf{H}_t\right\} \\ \mathbf{R}_{\mathbf{W_t}} = E\left\{\mathbf{W}_t^H \mathbf{W}_t\right\} \end{cases} \tag{12}$$

Then we can get $h(\mathbf{Y}_t | \mathbf{X}_t)$ as:

$$\begin{aligned} h\left(\mathbf{Y}_t | \mathbf{X}_t\right) &= MK \ln(\pi) + MK \\ &\quad + M \ln\left[\det\left(\mathbf{X}_t^H \mathbf{R}_{\mathbf{H}_t} \mathbf{X}_t + \mathbf{R}_{\mathbf{W}_t}\right)\right] \end{aligned} \tag{13}$$

Similarly, $h(\mathbf{W}_t)$ is:

$$h\left(\mathbf{W}_t\right) = MK \ln(\pi) + MK + M \ln\left[\det\left(\mathbf{R}_{\mathbf{W}_t}\right)\right] \tag{14}$$

Taking formulas (13) and (14) into formula (9), we can get:

$$I\left(\mathbf{Y}_t; \mathbf{H}_t | \mathbf{X}_t\right) = M \ln\left(\frac{\det\left(\mathbf{X}_t^H \mathbf{R}_{\mathbf{H}_t} \mathbf{X}_t + \mathbf{R}_{\mathbf{W}_t}\right)}{\det\left(\mathbf{R}_{\mathbf{W}_t}\right)}\right) \tag{15}$$

$I(\mathbf{Y}_t; \mathbf{H}_t|\ \mathbf{X}_t)$ is a measure of the amount of information transmitted between the transmitter and the receiver. The greater the MI, the greater the amount of information obtained from the target and the more accurate the detection. Therefore, in order to improve the detection ability of the target, it is necessary to make MI reach the maximum value. Thus the first optimization objective function is:

$$F_1 = \max I\left(\mathbf{Y}_t; \mathbf{H}_t|\mathbf{X}_t\right) \tag{16}$$

It can be seen from formula (15) that when the number of MIMO radars and the signal form are determined, and the environmental noise is basically unchanged, the main factor affecting the objective function F_1 is $\mathbf{R}_{\mathbf{H}_t}$.

Combined with formula (7), it can be seen that the factors that we control and can affect $\mathbf{H}_t$ are the position of our aircraft $\mathbf{P}_m = \left[x_{pm}^t, y_{pm}^t\right]$, and the energy P_{iu}^t used by each transmitter to detect each aircraft. At the same time, the transmitter needs to satisfy formula (3), which is the condition of energy constraint, and rewrite it into the matrix form as:

$$tr\left[\mathbf{X}_t^H \mathbf{X}_t\right] \leq P_0 \tag{17}$$

Therefore, the position of our aircraft and the corresponding radiated power can be adjusted at all times to maximize the amount of MI between the received echo and the transmitted signal, thereby improving the overall detection efficiency of the MIMO radar.

B. MI OF SIGNAL ECHOES AT ADJACENT TIME

Radar detection is actually a process of acquiring and accumulating information. If the radar gains more information about the target at the next moment, the detection effect will be significantly improved. If the information obtained by the two detection is the same, that is, there is almost no information gain (IG), the second detection has little effect.

In order to obtain a larger information increment, as much as possible, the acquired new information is orthogonal to the original information, and the independence of the two detection signals is improved, so that the amount of information acquired is extremely large. If the correlation of information is low during the two detections, it can be considered that the information orthogonality of the two detections is good. The lower the MI, the smaller the correlation between the two radar detections is. Therefore, this paper hopes that in the two consecutive detection processes, that is, the MI obtained by detection at time t and $t+1$ is the smallest, so as to achieve a good detection effect.

According to the formula of MI, the MI of radar echo at time t and $t+1$ can be expressed as:

$$\begin{aligned} I\left(\mathbf{Y}_t, \mathbf{Y}_{t+1}\right) &= h\left(\mathbf{Y}_t|\mathbf{X}_t\right) + h\left(\mathbf{Y}_{t+1}|\mathbf{X}_{t+1}\right) \\ &\quad - h\left(\mathbf{Y}_t\mathbf{Y}_{t+1}|\mathbf{X}_t\mathbf{X}_{t+1}\right) \end{aligned} \tag{18}$$

where $h(\mathbf{Y}_t|\ \mathbf{X}_t)$ is shown in the previous formula (13). Similarly, $h(\mathbf{Y}_{t+1}|\ \mathbf{X}_{t+1})$ can be expressed as:

$$\begin{aligned} &h\left(\mathbf{Y}_{t+1}|\mathbf{X}_{t+1}\right) \\ &= MK\ln(\pi) + MK \\ &\quad + M\ln\left[\det\left(\mathbf{X}_{t+1}^H \mathbf{R}_{\mathbf{H}_{t+1}} \mathbf{X}_{t+1} + \mathbf{R}_{\mathbf{W}_{t+1}}\right)\right] \end{aligned} \tag{19}$$

$$\begin{aligned} &h\left(\mathbf{Y}_t\mathbf{Y}_{t+1}|\mathbf{X}_t\mathbf{X}_{t+1}\right) \\ &= 2MK\ln(\pi) + 2MK \\ &\quad + M\ln\left[\det\left(\mathbf{X}_t^H \mathbf{R}_{\mathbf{H}_t} \mathbf{X}_t + \mathbf{R}_{\mathbf{W}_t}\right)\right] \\ &\quad + M\ln\left[\det\left(\mathbf{X}_{t+1}^H \mathbf{R}_{\mathbf{H}_{t+1}} \mathbf{X}_{t+1} + \mathbf{R}_{\mathbf{W}_{t+1}}\right)\right] \\ &\quad + M\ln\left\{\det\left\{\mathbf{I}_{N\times N} - \left[\mathbf{D}^{(t,t+1)}\right]^2\right\}\right\} \end{aligned} \tag{20}$$

where $\mathbf{I}_{N\times N}$ is the $N\times N$ dimensional identity matrix. $\mathbf{D}^{(t,t+1)}$ is the diagonal matrix obtained by singular value decomposition (SVD) of the covariance matrix $\mathbf{R}_{\widehat{\mathbf{Y}}_t\widehat{\mathbf{Y}}_{t+1}}$, expressed as:

$$\begin{aligned} \mathbf{R}_{\widehat{\mathbf{Y}}_t\widehat{\mathbf{Y}}_{t+1}} &= \mathrm{E}\left\{\widehat{\mathbf{Y}}_t^H \widehat{\mathbf{Y}}_{t+1}\right\} \\ &= \mathrm{E}\left\{\left(\mathbf{Y}_t\sqrt{\mathbf{R}_{\mathbf{Y}_t}^{-1}}\right)^{\mathrm{H}} \mathbf{Y}_{t+1}\sqrt{\mathbf{R}_{\mathbf{Y}_{t+1}}^{-1}}\right\} \\ &= \left(\sqrt{\mathbf{R}_{\mathbf{Y}_t}^{-1}}\right)^{\mathrm{H}} \mathbf{R}_{\mathbf{Y}_t\mathbf{Y}_{t+1}}\sqrt{\mathbf{R}_{\mathbf{Y}_{t+1}}^{-1}} \end{aligned} \tag{21}$$

where,

$$\mathbf{R}_{\mathbf{Y}_t\mathbf{Y}_{t+1}} = E\left\{\mathbf{Y}_t^H \mathbf{Y}_{t+1}\right\} \tag{22}$$

According to the above process, the result of formula (18) can be calculated as:

$$\begin{aligned} I\left(\mathbf{Y}_t, \mathbf{Y}_{t+1}\right) &= -M\ln\left\{\det\left\{\mathbf{I}_{N\times N} - \left[\mathbf{D}^{(t,t+1)}\right]^2\right\}\right\} \\ &= -M\sum_{n=1}^{N}\ln\left\{\det\left\{1 - \left[d_n^{(t,t+1)}\right]^2\right\}\right\} \end{aligned} \tag{23}$$

where $d_n^{(t,t+1)}$ are the diagonal elements of the matrix $\mathbf{D}^{(t,t+1)}$ arranged in the descending order. Thus, the MI at time t and $t+1$ can be quantified. To make the detection at time $t+1$ obtain more information gain based on the time t. It is necessary to ensure that the MI of the two detections is the smallest, to ensure that more information increment is obtained at time $t+1$. Then the objective function is:

$$F_2 = \min I\left(\mathbf{Y}_t, \mathbf{Y}_{t+1}\right) \tag{24}$$

In order to minimize the formula (24), it can be seen in combination with the formula (7) and the above discussion. When the signal pattern and environmental noise are basically unchanged, the objective function F_2 can be minimized by adjusting the position and radiated power of our aircraft at time t and $t+1$. According to the position and radiated power of our aircraft at time t, the position and power of the next time are optimized. And when optimizing the position of the next moment, we need to consider the speed and angle constraints of our aircraft.

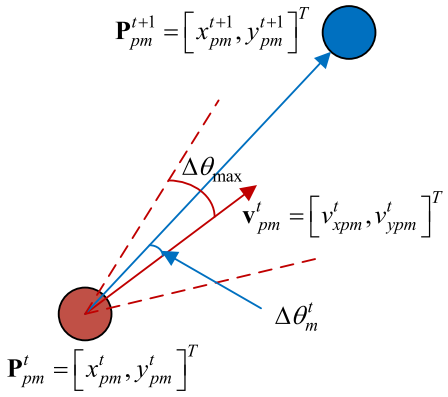

FIGURE 3. Schematic diagram on flight constraints.

C. FLIGHT CONSTRAINTS AND ENERGY CONSTRAINTS

During the optimization process, the relationship between the aircraft's track points is shown in Figure 3.

Suppose at time t, the position of our aircraft $\mathbf{P}_{pm}^{t} = \left[x_{pm}^{t}, y_{pm}^{t}\right]^T$ is shown by the red dot in the figure, and the speed is $\mathbf{v}_{pm}^{t} = \left[v_{xpm}^{t}, v_{ypm}^{t}\right]^T$. Through optimization, the position at the next moment is $\mathbf{P}_{pm}^{t+1} = \left[x_{pm}^{t+1}, y_{pm}^{t+1}\right]^T$, as shown by the blue dot in the figure. Then the speed constraint needs to be satisfied first, assuming that the time interval between the two moments is Δt. Then it should meet:

$$\begin{cases} \mathbf{P}_{pm}^{t+1} = \mathbf{P}_{pm}^{t} + \mathbf{v}_{pm}^{t}\Delta t \\ \left\| \mathbf{P}_{pm}^{t+1} - \mathbf{P}_{pm}^{t} \right\|_2 \le \left\| \mathbf{v}_{pm}^{t} \right\|_2 \Delta t \end{cases} \tag{25}$$

$\|\|_2$ means take the 2 norm. The distance between the two points should not be greater than the maximum distance the aircraft can fly in Δt. The speed at the this moment is $\mathbf{v}_{pm}^{t}$, which can be expressed as:

$$\mathbf{v}_{pm}^{t} = \mathbf{v}_{pm}^{t-1} + \Delta\mathbf{v}_{pm}^{t} \tag{26}$$

Then the constraints that formula (26) needs to satisfy are:

$$\begin{cases} \left\| \Delta\mathbf{v}_{pm}^{t} \right\|_2 \le \Delta v_{\max} \\ v_{\min} \le \left\| \mathbf{v}_{pm}^{t} \right\|_2 \le v_{\max} \end{cases} \tag{27}$$

That is, the speed $\left\| \Delta\mathbf{v}_{pm}^{t} \right\|_2$ of the aircraft adjustment should not exceed the maximum adjustable range $\Delta v_{\max}$. The adjusted speed $\left\| \mathbf{v}_{pm}^{t} \right\|_2$ cannot exceed its own speed range.

The course of an aircraft can be represented by a speed vector, as shown by the red arrow in the figure. The displacement of the aircraft within Δt can be obtained by subtracting two points, as shown by the blue straight line in the figure. The angle $\Delta\theta_m^t$ between the two straight lines is calculated by the angle between the vectors. Assuming that the maximum heading angle $\Delta\theta_{\max}$ that the aircraft can adjust is, the angle constraint is:

$$\left| \Delta\theta_m^t \right| \le \Delta\theta_{\max} \tag{28}$$

where $||$ means take the absolute value, the above-mentioned flight constraints are the limiting conditions in the optimization process. At the same time, the limiting conditions also include the energy limiting condition of formula (17).

D. TARGET STATE ESTIMATION BASED ON TRACK EXTRAPOLATION

In the above derivation and optimization of the target function, the core parameters $\mathbf{R}_{\mathbf{H}_t}$ and $\mathbf{R}_{\mathbf{H}_{t+1}}$ are not only related to the position and energy of our aircraft, but also to the position $\mathbf{T}_u^t = \left[x_{Tu}^t, y_{Tu}^t\right]^T$ and $\mathbf{T}_u^{t+1} = \left[x_{Tu}^{t+1}, y_{Tu}^{t+1}\right]^T$ at the time t and $t+1$ of the target aircraft. But obviously, it is impossible to obtain the position of the target before transmitting the signal. That is, when optimizing at time t, the position of the target $\mathbf{T}_u^t = \left[x_{Tu}^t, y_{Tu}^t\right]^T$ is unknown, and at the same time, the target position $\mathbf{T}_u^{t+1} = \left[x_{Tu}^{t+1}, y_{Tu}^{t+1}\right]^T$ at time $t+1$ cannot be obtained based on the echo at time t.

The MIMO radar can use the previous measured values and use Kalman filtering to predict the trajectory to obtain the target's estimated value $\tilde{\mathbf{T}}_u^t = \left[\tilde{x}_{Tu}^t, \tilde{y}_{Tu}^t\right]^T$ and $\tilde{\mathbf{T}}_u^{t+1} = \left[\tilde{x}_{Tu}^{t+1}, \tilde{y}_{Tu}^{t+1}\right]^T$. This technology is relatively mature in radar and will not be described here. After obtaining the estimated value of the target, the estimated $\mathbf{R}_{\tilde{\mathbf{H}}_t}$ and $\mathbf{R}_{\tilde{\mathbf{H}}_{t+1}}$ can be calculated. Approximately replace $\mathbf{R}_{\mathbf{H}_t}$ and $\mathbf{R}_{\mathbf{H}_{t+1}}$, and then optimize the position and radiated power at the next moment.

IV. OPTIMIZATION OBJECTIVE FUNCTION

In the above process, it involves maximizing the F_1 at time t, and minimizing the MI F_2 at the adjacent time. On the whole, although both of them are related to the position and power of our aircraft, considering the algorithm efficiency and computing speed, when optimizing its two objective functions, the two objective functions F_1 and F_2 can be time-shared Optimize or optimize at the same time.

A. TIME-SHARING OPTIMIZATION METHOD

The process of the time-sharing optimization method is that after obtaining the position $\mathbf{P}_p^t = \left[\mathbf{P}_{p1}^t, \mathbf{P}_{p2}^t, \ldots, \mathbf{P}_{pM}^t\right]$ of our aircraft and the estimated target position $\tilde{\mathbf{T}}_U^t = \left[\tilde{\mathbf{T}}_{T1}^t, \tilde{\mathbf{T}}_{T2}^t, \ldots, \tilde{\mathbf{T}}_{TU}^t\right]$ at time t, F_1 is optimized at that time. The optimization goals and constraints at this time are:

$$\begin{aligned} F_1 &= \max I\left(\mathbf{Y}_t; \mathbf{H}_t | \mathbf{X}_t\right) \\ &s.t.\ tr\left[\mathbf{X}_t^H \mathbf{X}_t\right] \le P_0 \end{aligned} \tag{29}$$

Using the position of our aircraft as a known quantity, we only optimize the power of each transmitter of our MIMO radar at time t, so that the MI between the transmitter and the receiver is the largest.

After optimizing to obtain the radiated power $P_{iu,opt}^t$ allocated to each target by each transmitter at time t, use it as a known quantity, and combine the measured target position $\mathbf{T}_U^t = \left[\mathbf{T}_{T1}^t, \mathbf{T}_{T2}^t, \ldots, \mathbf{T}_{TU}^t\right]$ at time t with the position information of our aircraft. According to the objective function

F_2, optimize the position of our aircraft. The corresponding optimization and constraints are:

$$F_2 = \min I\left(\mathbf{Y}_t, \mathbf{Y}_{t+1}\right) \quad s.t. \begin{cases} \left\| \mathbf{P}_{pm,opt}^{t+1} - \mathbf{P}_{pm}^{t} \right\|_2 \le \left\| \mathbf{v}_{pm}^{t} \right\|_2 \Delta t \\ \left\| \Delta \mathbf{v}_{pm,opt}^{t} \right\|_2 \le \Delta v_{\max} \\ v_{\min} \le \left\| \mathbf{v}_{pm}^{t} \right\|_2 \le v_{\max} \\ \left| \Delta \theta_m^t \right| \le \Delta \theta_{\max} \end{cases} \tag{30}$$

By optimizing the above objective function, the position of our aircraft can be obtained, and by using the corresponding relationship between position and speed in formula (25), the speed adjustment can be obtained to determine whether the above constraint conditions are met, and the decision is executed if it is satisfied. Thereby we can obtain the position $\mathbf{P}_{p,opt}^{t+1} = \left[\mathbf{P}_{p1,opt}^{t+1}, \mathbf{P}_{p2,opt}^{t+1}, \ldots, \mathbf{P}_{pM,opt}^{t+1}\right]$ of our plane at time $t+1$.

After obtaining the position of our aircraft at time $t+1$, iterative iterations are implemented to achieve continuous optimization. The corresponding time-sharing optimization process is shown in Figure 4.

The process is relatively intuitive and clear. Combining the above and the flowchart can achieve a time-sharing optimization for the allocation of detection resources, which will not be discussed in detail here.

The purpose of the initial state let $t = 2$ is to obtain the rough information of the target before further planning. The final termination condition is to judge whether the termination time t_e is reached.

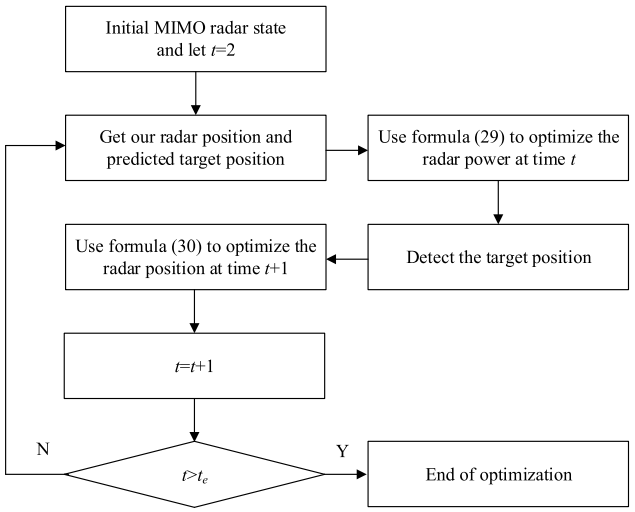

FIGURE 4. Flow chart of time-sharing optimization algorithm.

B. SIMULTANEOUS OPTIMIZATION METHOD

Simultaneous optimization method is to obtain the position information of our side and the target at time t, our radiation strategy, and to obtain the target position $\tilde{\mathbf{T}}_U^{t+1} = \left[\tilde{\mathbf{T}}_{T1}^{t+1}, \tilde{\mathbf{T}}_{T2}^{t+1}, \ldots, \tilde{\mathbf{T}}_{TU}^{t+1}\right]$ after one-step prediction, to optimize the radiation strategy and corresponding spatial position of our aircraft at time $t+1$. The corresponding optimization and constraints are:

$$F = \max\left(F_1 - F_2\right) \quad s.t. \begin{cases} tr\left[\mathbf{X}_{t+1}^H \mathbf{X}_{t+1}\right] \le P_0 \\ \left\| \mathbf{P}_{pm,opt}^{t+1} - \mathbf{P}_{pm}^{t} \right\|_2 \le \left\| \mathbf{v}_{pm}^{t} \right\|_2 \Delta t \\ \left\| \Delta \mathbf{v}_{pm,opt}^{t} \right\|_2 \le \Delta v_{\max} \\ v_{\min} \le \left\| \mathbf{v}_{pm}^{t} \right\|_2 \le v_{\max} \\ \left| \Delta \theta_m^t \right| \le \Delta \theta_{\max} \end{cases} \tag{31}$$

Combining the above objective function and constraints, we can complete the joint optimization of our radar position and radiated power at time $t+1$. After loop iteration, continuous planning can be achieved. The specific process is shown in Figure 5.

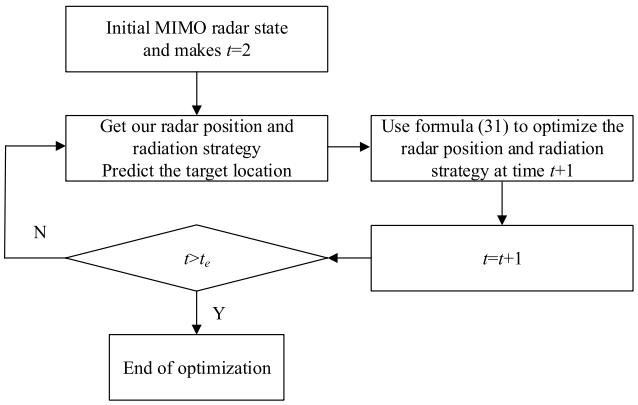

FIGURE 5. Flow chart of simultaneous optimization algorithm.

Through the above process, simultaneous optimization method for the allocation of radar detection resources can be completed.

It can be seen by comparing the time-sharing and simultaneous optimization algorithms that both of them depend on the original parameters by one-step prediction to obtain the target's possible position at the next moment. It is equivalent to relying on less accurate information for optimization. According to Figures 4 and 5, it can be seen that the time-sharing optimization algorithm optimizes the $M \times T$ radiated power matrix at time t. After the target is detected, more accurate target information is obtained, and then the coordinate matrix of $M \times 2$ at time $t+1$ is optimized. While simultaneous optimization method is based on fuzzy information and jointly optimizes the radiated power and the coordinate matrix, which is equivalent to optimizing the $M \times (T+2)$ dimension matrix.

Although the simultaneous optimization method can achieve joint optimization of energy and position, through the above discussion, the detection efficiency may be weaker than the time-sharing optimization method. And the target

dimensions to be optimized by the two are $M \times T$ and $M \times T + M \times 2$, respectively. For multivariable optimization problems, adding one parameter for optimization will exponentially increase the amount of calculation. Therefore, the calculation amount of the simultaneous optimization algorithm is higher than that of the time-sharing optimization algorithm.

In summary, this paper uses the time-sharing optimization algorithm to optimize the MIMO radar parameters. In the subsequent simulation part, a comparison of the two optimization methods will also be given, proving that the performance and speed of the time-sharing optimization algorithm are better than the simultaneous optimization algorithm.

C. OPTIMIZATION OF CONTINUOUS TIME SERIES

It can be seen from the above discussion and observations in Figure 4 and 5 that the optimization of the radiated power and position status of the MIMO radar is a continuous time series optimization problem. That is, the optimization result at time t is the initial state of optimization at time $t + 1$.

What this article wants to solve is a continuous time series optimization problem. If the value of the time interval Δt between the two times is small, although the initial states at t and $t + 1$ are different, the difference is small. Therefore, the optimization result at time t may be similar to the optimization result at time $t + 1$.

That is, if the optimization parameters at time $t + 1$ are initialized based on the optimization results at time t, good results may be achieved and a large amount of calculation time may be reduced. This is also an aspect of the follow-up article to improve the optimization algorithm. That is, the next optimization is to search near the optimization result, so as to realize the optimization of MIMO radar detection resources more quickly.

At the same time, considering the practical application background of this paper, this paper is a many-to-many cooperative air detection. Both parties are moving at high speed. Therefore, the real-time requirements of the algorithm are obviously stronger than the accuracy. In the case of limited airborne computing resources, the algorithm in this paper needs a feasible solution or a local optimal solution more than a global optimal solution. That is, according to the actual situation, the algorithm of this paper does not have high requirements for the accuracy of the results, but has higher requirements for the real-time performance of the algorithm. This also confirms that the article in the previous section prefers to use a time-sharing optimization algorithm with less calculation.

In summary, this paper needs an algorithm that can optimize the last optimization result as the initial state and has a faster speed. Therefore, this paper improves the applicability of the ABC algorithm to meet the algorithm's demand for the algorithm as much as possible.

V. IMPROVED ABC ALGORITHM

This section first introduces the principle and basic mathematical model of the ABC algorithm. Afterwards, based on the existing literature on improving ABC, this article perfects the improvement methods of previous scholars and builds a more complete search strategy, thereby enhancing the effectiveness of the ABC algorithm. Finally, for the allocation of MIMO radar detection resources, combined with the biological principle of the ABC algorithm, the ABC algorithm is adaptively improved to make it more suitable for solving the problems in this article.

A. ABC ALGORITHM

Artificial bee colony algorithm is a swarm intelligence algorithm proposed to simulate the behavior of honeybees. In ABC, there are three groups of bees constituting the whole colony—employed bees, onlookers, and scouts. First, employed bees search for honey sources and pass the information to onlookers. Then, onlooker made a selection of high-quality honey sources based on the information for further search. If the quality of the honey source does not improve after a certain period of search, the employed bees are converted to scout and a new honey source is searched again.

The corresponding algorithm flow can be described as follows:

Step 1: Initialize the population. Generate the first generation population of $BN \times D$ dimension. Where BN is the number of populations and D is the dimension of the search space.

$$\begin{bmatrix} x_{1,1}^1 & x_{1,2}^1 & \cdots & x_{1,D}^1 \\ x_{2,1}^1 & x_{2,2}^1 & \cdots & x_{2,D}^1 \\ \vdots & \vdots & \ddots & \vdots \\ x_{BN,1}^1 & x_{BN,2}^1 & \cdots & x_{BN,D}^1 \end{bmatrix} \tag{32}$$

For the initial parameters of the i-th solution $\mathbf{X}_i^1 = \left[x_{i,1}^1 \; x_{i,2}^1 \cdots x_{i,D}^1 \right]$, each of $x_{i,j}$ is generated by formula (33).

$$x_{i,j}^1 = x_{\min,j}^1 + r\left(x_{\max,j}^1 - x_{\min,j}^1 \right) \tag{33}$$

where $i = 1, 2, \ldots, BN$, $j = 1, 2, \ldots, D$, $x_{\max,j}^1$ and $x_{\min,j}^1$ are the lower and upper bounds of the j-th dimension. r is a random number with uniform distribution between (0,1).

Step 2: The employed bees started searching. Use formula (34) to search and obtain the candidate solution $v_{i,j}^{n+1}$ of the $(n + 1)$-th iteration.

$$v_{i,j}^{n+1} = x_{i,j}^n + \phi\left(x_{i,j}^n - x_{k,j}^n \right) \tag{34}$$

where n and $n + 1$ represent the number of iterations, $n = 1, 2, \ldots, N$, k is the positive integer with uniform random values in $[1, BN]$, ϕ is a random number with uniform distribution between $(-1, 1)$. Use $\mathbf{V}_i^{n+1} = \left[v_{i,1}^{n+1} \; v_{i,2}^{n+1} \cdots v_{i,D}^{n+1} \right]$ and $\mathbf{X}_i^n$ to calculate the corresponding fitness function $F\left(\mathbf{V}_i^{n+1} \right)$ and $F\left(\mathbf{X}_i^n \right)$. Keep the better of the two and the corresponding parameters for the next iteration.

Step 3: Onlooker chooses honey source. Onlooker uses roulette to select honey sources for further exploration. The

way of roulette is:

$$P_i^n = \frac{F\left(\mathbf{X}_i^n\right)}{\sum_{i=1}^{BN} F\left(\mathbf{X}_i^n\right)} \tag{35}$$

where P_i^n is the probability that onlooker will choose $\mathbf{X}_i^n$ after the n-th search. Obviously, the better the fitness function, the greater the corresponding probability, so that it is easier to concentrate the advantageous resources to search near the point and obtain better optimization results.

Step 4: The employed bee is converted to scout. If after the set number of searches, the fitness of the i-th employed bee search result has not improved. Then convert the employed bee to scout. Starting again from Step 1, a new solution is randomly produced by the scout to replace the old one.

The above process is the core step of the ABC algorithm. The algorithm has strong search performance, and because of its few parameters and easy implementation, it is widely used in many fields. But the ABC algorithm itself still has room for improvement. Therefore, the next two sections of this article will improve the ABC algorithm level to improve the efficiency of the algorithm. And the adaptive improvement combined with the problems required in this paper makes it more suitable for solving the problem of MIMO radar detection resource allocation constructed in this paper.

B. ABC ALGORITHM IMPROVEMENT

In order to improve the performance of the ABC algorithm, this section improves the ABC algorithm in terms of improving the search direction and constructing a three-level search strategy.

1) IMPROVE SEARCH DIRECTION

Observing formula (34) and Step 2, we can see that due to the positive and negative randomness of ϕ, the search direction has randomness. It is very likely that the newly generated candidate solution $v_{i,j}^{n+1}$ has poor performance. If the transformation direction of the function can be changed in the direction of improving the fitness function, more computing resources will be saved, thereby improving the efficiency of the algorithm. Therefore, the literature [38] rewrites the formula (34) as:

$$v_{i,j}^{n+1} = x_{i,j}^n + \sigma_{i,j}^n \left|\phi_{i,j}^n\right| \left|x_{i,j}^n - x_{k,j}^n\right| \tag{36}$$

where $\sigma_{i,j}^n$ and $\left|\phi_{i,j}^n\right|$ represent the search direction and search step respectively, so that the search direction can be directly controlled by controlling the sign of $\sigma_{i,j}^n$. This method is to make $\sigma_{i,j}^n$ take a random value only between $+1$ and -1 two values, and calculate $v_{i,j}^{n+1}$ after the random value. If the fitness function $f\left(v_{i,j}^{n+1}\right)$ corresponding to $v_{i,j}^{n+1}$ is better than $f\left(x_{i,j}^n\right)$, it is considered that the search direction is better and the subsequent calculation is continued. If the performance function is worse than $f\left(x_{i,j}^n\right)$, let $\sigma_{i,j}^n$ take the opposite number and perform subsequent operations.

Through the improvement of [38], the algorithm efficiency can be significantly improved. However, in the two cases of finding near the maximum value or the initial value the minimum value, the effect of this strategy may be limited.

For a more detailed explanation, this paper selects the function of formula (37) in the interval [0, 10], and the corresponding function curve is shown in Figure 6.

$$y = -0.1x^3 + 0.5x^2 + 0.3x + 5 \tag{37}$$

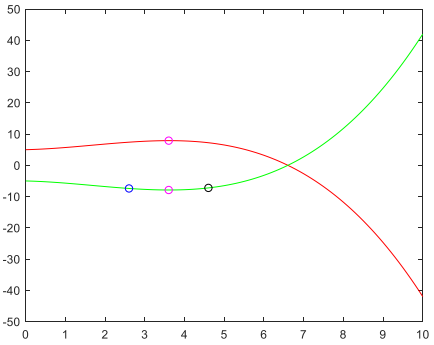

FIGURE 6. Example function curve.

Suppose x is an independent variable and y is a fitness function. The red curve in Figure 6 is the curve corresponding to formula (37), and the green curve is the $-y$ curve. The pink point on the red curve is the maximum value of the fitness function y value in this area ($x = 3.6$, $y = 7.894$). That is, the optimization process at this time reaches the local best. At this time, according to the method of [38], no matter how $\sigma_{i,j}^n$ is taken, the fitness function will decrease, and the next search will return to this point. This repeated search has no effect. Therefore, when the maximum value is searched, it is impossible to calculate only one direction. Similarly, when the search is near the local best point and the next search step is large, the above situation will also occur. This situation is relatively common, so the algorithm of [38] needs to be improved.

The improvement method for the above situation is not to calculate only one direction, but to calculate the two directions and compare. If the performance is degraded in both directions, it means that it is likely that the extreme advantage has been searched at this time. After narrowing the search step, search is performed. If the fitness function is still not improved after continuously reducing the step size, let $\sigma_{i,j}^n = 0$, that is, stop searching. If the performance is improved in both directions, it means that it may be near the poor point at this time. At this time, compare the degree of improvement in both directions. Select the direction with the better improvement to search.

Thus, the completion of the method of [38] is completed.

2) CONSTRUCT A THREE-LEVEL SEARCH STRATEGY

Observing formula (34), we can see that the search strategy of the classic ABC algorithm is relatively random, which is also

the main reason why the ABC algorithm is often evaluated as aimless and inefficient [39], [40], and it is also the main point for scholars to improve the ABC algorithm.

Reference [41] was inspired by an improved particle swarm optimization algorithm and designed an elite search strategy. That is, in the search process, consider the influence of the best point of the global in history and the best point of the current. Two search methods were designed, namely:

$$v_{i,j}^{n+1} = x_{r,j}^{n} + \lambda\left(x_{i,j}^{n} - x_{r,j}^{n}\right) + \mu\left(x_{best,j} - x_{r,j}^{n}\right) \tag{38}$$

$$v_{i,j}^{n+1} = x_{best,j} + p_n\left(x_{i,j}^{n} - x_{best,j}\right) + \alpha\left(x_{r,j} - x_{best,j}\right) \tag{39}$$

$x_{r,j}^{n}$ represents the j-th dimension of historical optimal solution of the bee. $x_{best,j}$ represents the j-th dimension of the current global optimal answer. p_i denotes the possibility that the current n-th employed bee will be selected by the onlooker, α, λ and μ represent the corresponding random coefficients.

This method generates new search points near the global best point, and then search in the direction of the global history best point, which has a better search efficiency than the classic ABC method. However, if only the influence of the global best is considered, the possibility of falling into the local optimum is increased.

For a more detailed explanation, this paper selects the function of formula (40) in the interval [0, 20], and the corresponding function curve is shown in Figure 7.

$$y = x\sin(2\pi x) \tag{40}$$

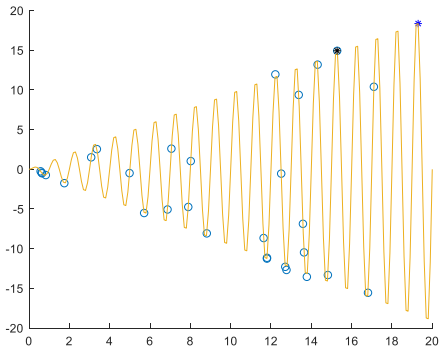

FIGURE 7. Example function curve.

Suppose the initial state is shown in the blue circle in the figure. Use the method of [41] to find the optimal value of this function. Then the global best advantage found at this time is the point corresponding to the black * in the figure. If we search according to formulas (38) and (39), all the blue circles will move toward the black point and eventually converge to that point. But obviously, the best advantage of this function is in the position corresponding to the blue * on the right side of the figure. That is, if it has been moving in the direction of the black dot, the possibility of the algorithm converging to the local best has increased.

Therefore, it is necessary for bees to conduct random searches. But continuous random search will waste a lot of computing resources. A compromise method can be used to allow bees to conduct random searches early to increase the diversity of the population and reduce the possibility of falling into a local optimum.

Inspired by reference [41], elite strategies can be constructed to search, thereby improving the efficiency of the algorithm. And the elite can be composed of a global optimal solution and multiple local optimal solutions, which together affect the search. That is, group the bees, and in the search process, add the influence of the current optimal solution x_{lbest}^{n} and the historical optimal solution x_{lbest} in each group to improve the search effect.

This paper uses system clustering method to group bees, make the bees that are closer to be divided into a group, and search a certain area together. System clustering is mature in theory and has stable source code in MATLAB. Here is not too much introduction to the principle of the algorithm. However, the system clustering method needs to define the number of groups. In this paper, the number of groups is the same as the number of local elites. In the following text, the number of elites is $\lceil 0.05BN \rceil$, that is, 5% of the population, and bees can be grouped, where $\lceil\rceil$ represents the arithmetic method of rounding up. Assuming that there are 50 bees in the population, the result is 3, that is, 50 bees are divided into three groups.

Therefore, the improved search strategy of this article is:

$$v_{i,j}^{n+1} = \begin{cases} x_{i,j}^{n} + \phi_1\left(x_{i,j}^{n} - x_{k,j}^{n}\right) \\ \qquad 0 < n < 0.2BN \\ x_{i,j}^{n} + \dfrac{n}{BN}\left[\phi_2\left(x_{i,j}^{n} - x_{lbest}^{n}\right) + \phi_3\left(x_{i,j}^{n} - x_{lbest}\right)\right] \\ \qquad 0.2BN \le n < 0.7BN \\ x_{i,j}^{n} + \dfrac{n}{BN}\left[\phi_4\left(x_{i,j}^{n} - x_{gbest}^{n}\right) + \phi_5\left(x_{i,j}^{n} - x_{gbest}\right)\right] \\ \qquad 0.7BN \le n \le BN \end{cases} \tag{41}$$

where x_{gbest}^{n} and x_{gbest} represent the current global optimal solution and historical optimal solution. The ϕ_1 has been discussed in the previous section. ϕ_2 to ϕ_5 are random numbers that obey uniform distribution within (0,1).

In a total of BN searches, the bees within the first $0.2BN$ searches performed an improved random search strategy to expand the diversity of the bee colony.

In the middle of the search, the bees are grouped, and the bees in each group are affected by the optimal solution in the group. As the search proceeds, the local best may change, and the performance is getting better and better, and the impact should be greater and greater. Therefore, the coefficient n/BN is constructed to describe this effect. At the same time, in the middle of this step, that is, when $(0.2BN+0.7BN)/2=0.45BN$ times are searched, in order to prevent the bees from being far away due to movement, the system clustering method is used to regroup the bees to continue the search.

In the final stage of the search, the bees have conducted a more comprehensive and accurate search of the space. At this time, it is convenient to use the global best to guide the bees to search near the global best to obtain good search results.

Through the above improvements, the search efficiency of the ABC algorithm can be improved.

C. APPLICABILITY IMPROVEMENT FOR MIMO RADAR DETECTION RESOURCE ALLOCATION

The core purpose of this article is to improve the detection efficiency of MIMO radar. In addition to improving the efficiency of the algorithm, we can also adjust the algorithm in accordance with the problem, we want to make it more suitable for the problem to be optimized and get a better optimization result.

Therefore, this article adapts ABC from the following three aspects.

1) INITIALIZE THE NEXT GENERATION POPULATION BASED ON THE RESULTS OF THIS OPTIMIZATION

The allocation of MIMO radar detection resources is a continuous time series planning problem. If the time interval Δt between the two time series is small. Considering the motion constraints of both aircrafts, it is likely that the states of our aircrafts and targets have not changed significantly at t and $t + \Delta t$. That is to say, the parameters to be optimized are different between t and $t + \Delta t$, but the gap is small. It is likely that the results of optimization at these two moments are relatively similar.

Therefore, in the search process, the optimization result at time t can be used as the initial state of the $t + \Delta t$ bee colony to start optimizing, thereby improving the efficiency of the algorithm.

At the same time, the idea was also inspired by the biological characteristics of bees, that is, bees will search for new honey sources based on the previous honey sources. Compared with the previous search, the new search has a similar initial state and optimization goal. This allows we to optimize based on previous search results.

This is reflected in the algorithm that after completing the optimization at time t, the bee will obtain the historical optimal solutions x_{lbestk} of K groups during the optimization process at time t, $k = 1, 2, \ldots, K$, and at the same time will obtain the global historical optimal solution x_{gbest}. In the following, x_{lbestk} and x_{gbest} will be expressed uniformly as x_{best}. Then the formula (33) of ABC algorithm Step 1 can be adjusted to:

$$x_{i,j}^{1} = x_{best,j} + \gamma \left(x_{\max,j}^{best} - x_{\min,j}^{best} \right) \tag{42}$$

where γ is a random number that is uniformly distributed between $(-0.1, 0.1)$, $x_{\max,j}^{best}$ and $x_{\min,j}^{best}$ represent the maximum and minimum values of the j-th attribute in x_{best}. Formula (42) indicates that a historical optimal solution is randomly selected in x_{best}, and the next generation initial bee colony is generated near this optimal solution.

At the same time, the real-time requirements of the algorithm are considered, and this article hopes to get a feasible solution. Therefore, in the subsequent search, only bees with a population of $0.2BN$ are generated using formula (42). Combining the generated results with the optimal solution x_{best}, the new initial population can be obtained as:

$$\begin{bmatrix} x_{1,1}^{1} & x_{1,2}^{1} & \cdots & x_{1,D}^{1} \\ x_{2,1}^{1} & x_{2,2}^{1} & \cdots & x_{2,D}^{1} \\ \vdots & \vdots & \ddots & \vdots \\ x_{0.2BN,1}^{1} & x_{0.2BN,2}^{1} & \cdots & x_{0.2BN,D}^{1} \\ x_{lbest1,1}^{1} & x_{lbest1,2}^{1} & \cdots & x_{lbest1,D}^{1} \\ x_{lbest2,1}^{1} & x_{lbest2,2}^{1} & \cdots & x_{lbest2,D}^{1} \\ \vdots & \vdots & \ddots & \vdots \\ x_{gbest,1}^{1} & x_{gbest,2}^{1} & \cdots & x_{gbest,D}^{1} \end{bmatrix} \tag{43}$$

Through the above method, the inherited optimization result can be realized, thereby improving the search speed and efficiency of the algorithm.

However, it is obvious that if the above method falls into the local best when performing the global search for the first time, all subsequent optimization results are likely to fall into the local best. At the same time, in order to improve the real-time performance of the algorithm, the number of populations has been greatly reduce, resulting in subsequent optimization results may not be accurate. The use of the above method will cause this inaccuracy to accumulate gradually, and eventually degenerate from a better solution to a feasible solution or even no search results.

In order to avoid the above-mentioned problems, after a certain time of continuous planning, all parameters need to be emptied, and the algorithm re-planned to regenerate the optimal solution. This reduces the possibility of gradual performance degradation.

2) TERMINATION OF EMPLOYED BEE

In Step 4 of the ABC algorithm, if an employed bee searches multiple times and the performance of the search results does not improve, it is converted to scout.

In order to improve the real-time performance of the algorithm, this paper improves the process.

If the search efficiency of the employed bee is not improved, the subsequent optimization of the employed bee is directly stopped. And record the parameter set $\mathbf{X}_c$ and optimal solution $F(\mathbf{X}_c)$ corresponding to the employed bee. If the search for other employed bee finds a better solution, just discard $F(\mathbf{X}_c)$. However, if no better results appear until the end of all bee searches, it is judged whether $F(\mathbf{X}_c)$ is a feasible solution. If it is a feasible solution, it is directly used as the optimization result. Otherwise, use formula (42) and (43) to regenerate the population and search again.

This is because the subsequent search is based on the optimal solution at the previous moment. The employed bee search effect has not been improved, indicating that it has converged to the local optimal solution, and the search

performance is difficult to improve. If it is converted into a scout according to the ABC algorithm, it is likely that in the subsequent search process, the scout may not be able to obtain better results than it is now. This increases the complexity of the algorithm, and at the same time does not significantly improve performance.

The requirement of the algorithm in this paper is to be able to quickly optimize a better feasible solution. However, this paper does not need to consume a large amount of computing resources to obtain a global optimal solution. Therefore, the process of converting employed bee to scout contradicts the needs of this article. In order to optimize the MIMO radar resource allocation problem, this article directly stops the search for the employed bee and performs the subsequent operations described above.

3) IMPROVING POPULATION PARAMETERS AFTER DETERIORATING HONEY SOURCE

The optimization of the MIMO radar position is carried out by extrapolating the track to predict the position $\tilde{\mathbf{T}}_U^t = \left[\tilde{\mathbf{T}}_{T1}^t, \tilde{\mathbf{T}}_{T2}^t, \ldots, \tilde{\mathbf{T}}_{TU}^t\right]$ of the target. However, if a certain aircraft or a few aircrafts in the target group adjust the movement state, such as steering or acceleration, the predicted result will deviate greatly from the real result. Then, the prediction results with larger errors are used to perform optimization operations, which ultimately lead to a decrease in the performance of the optimization results.

When a large error occurs, first let Δt be half of the original. That is, the sampling frequency is increased to obtain more track points per unit time, which is convenient for prediction. At the same time, it can be seen from Figure 4 above that the time interval between prediction and actual detection is very short, and the error between the two can be obtained in real time.

Suppose that u_c targets among U targets have changed state. The algorithm needs to adjust γ in formula (42), as shown in formula (44).

$$\gamma_N = \gamma\left(1 + \frac{10u_c}{U}\right) \tag{44}$$

That is to allow bees to search in a larger area near the last optimal solution, thereby enhancing the population diversity of bees. At the same time, formula (42) is improved to generate new populations. The new population NBN is:

$$NBN = 0.2BN + 2\frac{u_c}{U}BN \tag{45}$$

That is, on the basis of the original, the population is supplemented according to the proportion to conduct a more accurate search.

Although there is an error, the error will not be large due to the target's own motion constraints. Therefore, the optimization results of the previous moment can still be used. By increasing the population diversity and population number, the ABC algorithm can conduct a more extensive search, and it can still find a better feasible solution. After multiple moments of optimization, the detection performance will return to optimal.

After the error between the prediction error and the detected value recovers to the allowable range, Δt is recovered.

VI. OPTIMIZATION PROCESS OF MIMO RADAR DETECTION RESOURCES BASED ON IABC

Combining with the improvement process of ABC above, the optimization process of MIMO radar detection resources based on the IABC algorithm is shown in Figure 8.

The process of Figure 8 can be summarized as the following steps.

Step 1: Initially obtain target state information at $t = 1$ and 2 and initial MIMO radar state parameters at $t = 3$.

Step 2: Obtain the position of the MIMO radar at this moment and predict the position of the target.

Step 3: Initialize the ABC initial parameters according to the optimization times. If it is the first time or the honey source is deteriorated, a random $BN\times D$ or $NBN\times D$ dimension first generation population is generated. Otherwise, the initial population of $(0.2BN+K+1)\times D$ dimension is generated according to the previous optimization results and formulas (42).

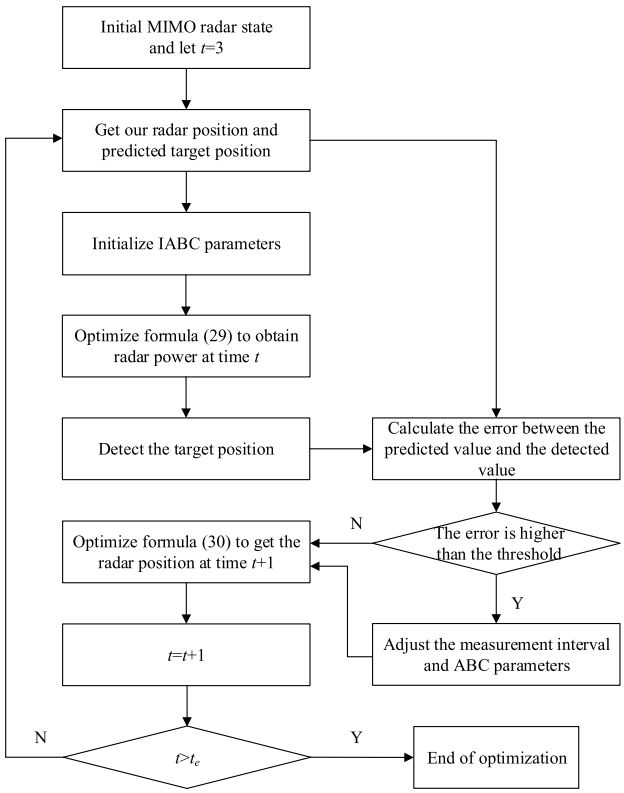

FIGURE 8. MIMO radar detection resource optimization flow chart based on IABC algorithm.

Step 4: Use IABC to optimize formula (29) to get the radar radiation strategy at this moment, and detect the measurement position of the target.

Step 5: Calculate the error between the measured position and the predicted position. If it is higher than the error threshold, that is, the prediction effect is poor, and some targets change the motion state, Step 6 is executed. Otherwise, go to Step 7.

Step 6: Adjust the measurement interval and ABC parameters according to the method of improving the population parameters after the honey source deteriorates.

Step 7: Use IABC to optimize formula (30) to obtain the optimal position of the radar at the next moment, and increase the counting parameter t by 1.

Step 8: Determine whether the specified end time t_e is reached, that is, whether the detection task ends. If not, return to Step 2. Otherwise, the detection optimization ends.

Through the above process, IABC can be used to dynamically optimize the allocation of MIMO radar detection resources.

VII. SIMULATION VERIFICATION

In this section, through three sets of Monte Carlo experiments, the effectiveness of this algorithm and the advantages of this model are compared and verified.

The first group is to compare the simultaneous optimization algorithm and the time-sharing optimization algorithm under the same initial parameters to verify that the time-sharing optimization algorithm has better advantages. The second group compares the time-sharing optimization algorithm designed in this paper with the algorithms corresponding to literature [15], [21], [30], respectively, to show that the model can improve the detection efficiency of radar. The third group is to compare the IABC in this article with the original ABC algorithm, the improved ABC algorithm corresponding to the literature [38] and [41], to optimize the MIMO radar parameters.

A. COMPARISON OF TWO OPTIMIZATION METHODS

In order to verify the advantages and feasibility of the proposed method, the proposed method is simulated and verified.

Suppose there are 3 targets in the space, namely Target1, Target2 and Target3. Suppose that the three targets fly from (50,76), (67,74) and (78,56) along a straight line to (30,56), (58,46), (100,36) at a uniform speed. There are 20 optimization points. The amplitude ratio of signal to noise is 0 dB. The three aircraft used for collaborative detection taking off from (0,0), (20,0) and (40,0), respectively, combined with flightability and energy constraints, to optimize the above objective function. The detection trajectories obtained by time-sharing optimization and simultaneous optimization are shown in Figure 9 and 10.

It can be seen from the comparison between Figure 9 and 10 that the trajectories of R1 and R3 are similar in the above two figures, and the corresponding power distributions are relatively similar, while the trajectory of R2 is different. The smaller the distance between our aircraft and the target group, the better the detection effect of our radar is. Comparing Figure 9 and 10, it can be seen that in the middle of the

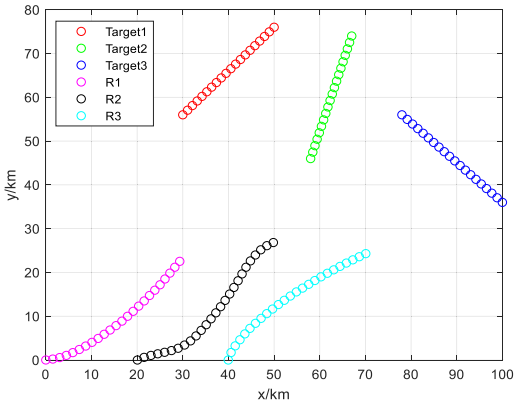

FIGURE 9. Time-sharing optimization algorithm.

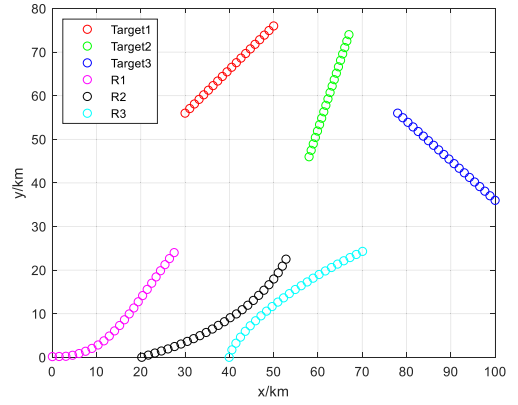

FIGURE 10. Simultaneous optimization algorithm.

flight, the slope of the black trajectory in Figure 9 is greater than that in Figure 10, R2 in Figure 9 approaches the target group faster, and the distance between the two sides decreases faster. In the final stage of detection, the R2 trajectory in Figure 9 points to Target3, while Figure 10 points to Target2. It can be seen from the figure that the distance between R2 and Target2 is already small, while the distance between R3 and Target3 is significantly increased. Therefore, in the final stage of detection, R2 uses part of the detection power to detect Target3, and moves toward Target3, which is beneficial to improve the overall detection efficiency. Therefore, it can be qualitatively determined that the time-sharing optimization method is superior to the simultaneous optimization method.

To further compare the performance of the two optimization methods, 30 Monte Carlo simulation experiments were performed on both methods, and the positioning of the Mean Squared Error (MSE) after each joint track and power optimization in the 30 simulations was recorded. As shown in Figure 11. At the same time, record the time for the two algorithms to complete a joint optimization, as shown in Figure 12.

It can be seen from Figure 11 that the positioning accuracy of the time-sharing optimization algorithm is better than that

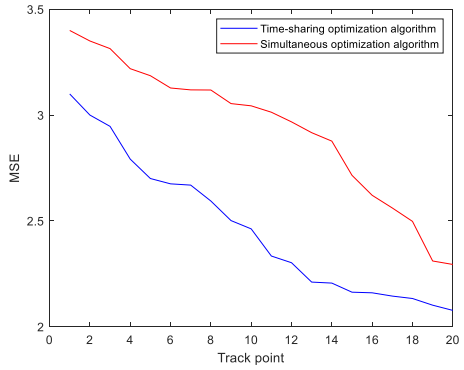

FIGURE 11. Comparison of errors.

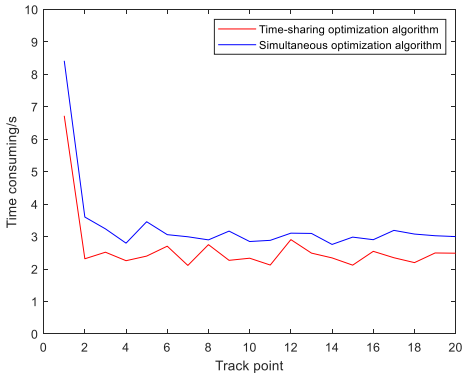

FIGURE 12. Comparison of optimization time.

of the simultaneous optimization algorithm. This is because in the initial stage, the distance between our aircraft and the target group is far, and the positioning error is large. This directly leads to a larger position error in predicting the target group at the next moment. The time-sharing optimization algorithm only needs to predict the position of the target at the current time, while the optimization algorithm needs to predict the position of the target at the current and next time, and the error will accumulate as the prediction step increases. That is, the initial error amount of the simultaneous optimization algorithm is always higher than the error amount of time-sharing optimization. Therefore, its positioning effect is weaker than the simultaneous optimization algorithm. Although this error will gradually decrease as the detection progresses, this is also the reason why the error of the simultaneous optimization algorithm in Figure 11 gradually decreases. However, due to the error of the initial parameters, the performance of the simultaneous optimization algorithm cannot always exceed the time-sharing optimization algorithm.

At the same time, it can be seen from Figure 12 that the time-sharing optimization algorithm has a faster algorithm speed. This is because for the optimization problem, the calculation amount and the parameter of the parameter to be optimized are not linearly related. It is usually a multiple or exponential relationship. Therefore, although time-sharing optimization has the same parameters as the simultaneous optimization method, time-sharing optimization can significantly reduce the amount of calculation and improve the efficiency of the algorithm.

In summary, the time-sharing optimization algorithm is superior to the simultaneous optimization in both algorithm accuracy and speed, which verifies the previous discussion. Subsequent time-sharing optimization is used to allocate MIMO radar detection resources.

B. COMPARISON OF DETECTION MODELS

To further compare the performance of the algorithm in this paper with other related algorithms, the algorithm in this paper is compared with the algorithms in [15], [21] and [30]. Since the algorithm in the literature does not involve the optimization of the spatial topology, this article assumes that the three aircraft are all flying at the same speed in the same direction, and their space trajectories are shown in Figure 13.

According to the spatial position shown in Figure 13, the algorithms in [15], [21] and [30] are used to optimize the radiated power and other related parameters to improve the detection efficiency of the corresponding airborne MIMO radar.

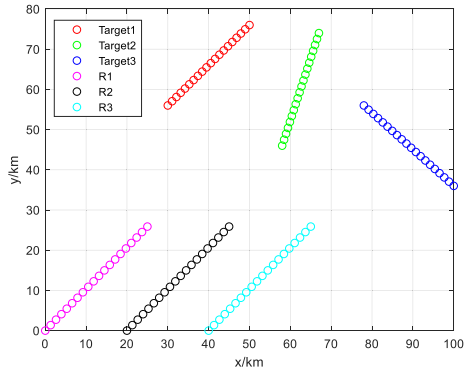

FIGURE 13. Fixed formation track.

In order to quantitatively compare the performance of the algorithm, the method of this paper and the above three algorithms were carried out in order 30 Monte Carlo simulation experiments. Using MSE as an evaluation index, compare the performance of the algorithm in this paper with the literature [15], [30]. The results are shown in Figure 14.

It can be seen from Figure 14 that the algorithm in this paper is superior to the algorithms in [15] and [30]. This is because compared with the algorithms in [15] and [30], this paper optimizes the spatial position of the radar, which makes the radar more flexible to adjust its position and improve the detection efficiency.

The reason why the algorithm in this paper is superior to the algorithm in [15] is because the objective function in [15] is posterior Cramer-Rao lower bound (PCRLB) in the worst case. Based on PCRLB, the allocation of radar radiation power and bandwidth is optimized. This method can obviously improve the lower limit of radar detection capability,

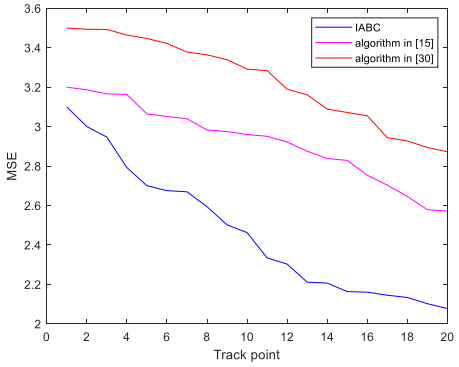

FIGURE 14. MSE comparison chart.

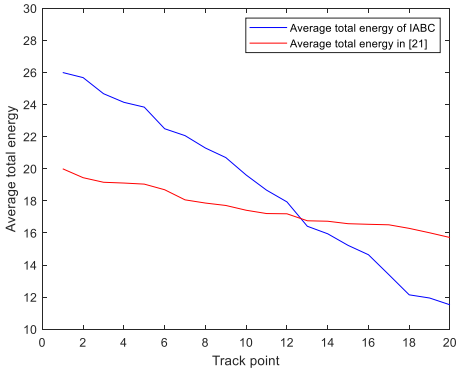

FIGURE 15. Comparison of the average power of each track point.

but it has a limited role in improving the radar detection capability under normal circumstances. It is like the government has adjusted the welfare policy to increase the income of the lowest income group. But for people with regular income, help is limited. At the same time, reference [15] designed the detector based on Neyman-Pearson criterion. The detector is not designed in combination with the predictor, and the detection efficiency is also limited. And the reference [15] is the PCRLB obtained under the condition of high signal-to-noise ratio, and this paper is verified under the condition of 0dB signal-to-noise ratio. Therefore, the performance of the algorithm in this paper is better than the algorithm in [15].

The reason why this paper is superior to literature [30] is that the algorithm in this paper minimizes the MI between the two received signals, and literature [30] also hopes to reduce the correlation between different radar perceptions to improve CS-based detection techniques. The goals of the two methods are similar. This article not only reduces the amount of MI, but also increases the MI between the transmitted and received signals. Compared with literature [30], more factors are considered, so the performance is better. And when the number of radars is small, the correlation between different radar echoes is not high. Therefore, the method of [30] is adopted under the simulation conditions in this paper, and the degree of improving radar detection capability is limited.

The optimization goal of [21] is to minimize the total power under the certain of signal-to-interference-plus-noise ratio (SINR) requirement. Therefore, in this paper, the SINR is set to 0dB, and 30 Monte Carlo experiments are recorded. Each track point corresponds to the average value of the total power. Compare the power allocation between the algorithm and the literature [21]. As shown in Figure 15.

It can be seen by comparing the two curves in Figure 15. In the initial stage, the method of [21] has obvious advantages. However, with the movement of our aircraft, the total power required by the method in this paper is obviously decreasing, and the follow-up is obviously less than the method in [21]. This is mainly due to two reasons. The first is that the radiated power is highly related to the distance between the two parties. The algorithm in this paper can significantly reduce the distance difference between the two sides by adjusting the position, thereby reducing the energy demand. The other reason is that this paper strives to maximize the MI between sending and receiving, so in the optimization process, it will try to reduce the impact of noise correlation, thereby reducing the demand for power. Although minimizing the MI at adjacent moments also has this effect, the effect is not obvious and should not be discussed as an important point. Therefore, the algorithm in this paper is superior to the algorithm in [21].

C. COMPARISON OF OPTIMIZATION ALGORITHMS

In order to compare the performance of the improved ABC algorithm in this paper, this section compares the improved ABC algorithm with the classic ABC, the improved ABC algorithm in literature [38] and literature [41]. The population number BN=100. The relevant parameters of the corresponding algorithm are the same as the values in the literature, and 30 Monte Carlo experiments are performed to obtain the error chart and algorithm time-consuming curve of different algorithms, as shown in Figure 16 and Figure 17. At the same time, in 30 Monte Carlo simulation experiments, a simulation curve is randomly selected, as shown by the solid black line in the figure.

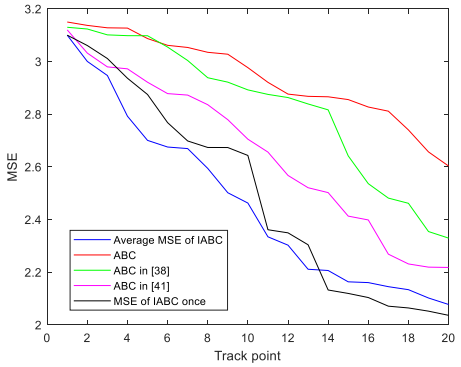

FIGURE 16. MES comparison chart.

It can be seen from the above comparison that from the perspective of MSE, the improved ABC algorithm in this paper is superior to other algorithms in both accuracy and

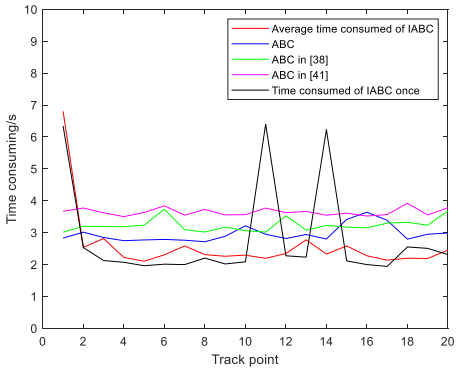

FIGURE 17. **Comparison of the average time consumption of the algorithm.**

speed. The improvement in accuracy is because this article is based on the classic ABC algorithm, drawing on the main ideas of [38] and [41] and improving it, optimizing the search direction and constructing a three-level search strategy to make the search range larger and the search also more precise. The improvement in speed is due to the improved applicability of the algorithm in this article. Make the first search a more time-consuming and laborious global search to obtain an excellent initial state. It can be seen from the figure that the search time of the improved ABC algorithm for the first time is significantly higher than the time of other algorithms, and the subsequent time-consuming is significantly less than other algorithms. This is because this article uses the current optimized solution constructed as the initial state of the next search, the method of reducing the number of bees and terminating part of the bee search directly improves the speed of subsequent searches.

The statistical characteristics of the algorithm in this paper are obviously superior to other algorithms, but the statistical characteristics weaken the characteristics of many algorithms themselves. Therefore, this paper supplements the error and time-consuming curve of an optional optimization in Figure 16 and 17.

In Figure 16, since there is an error in each measurement, the error accumulation leads to an increase in track prediction error. When the error gradually accumulates and reaches the state where the honey source deteriorates, the algorithm will give up the previous results and perform a new search. That is, the error of the black curve in Figure 16 suddenly decreases, and the algorithm in Figure 17 significantly increases in time, as shown by the 11th track point in the figure. As the algorithm continues, the re-search may occur again, that is, there may be a sudden drop in the black error curve in Figure 16 and a spike in the black time-consuming curve in Figure 17 again. As shown in the 14th track point. Because this kind of re-searching situation may happen at any time, while when calculating the average error and the time-consuming of the algorithm, the characteristics of this mutation are processed uniformly, which is difficult to reflect in statistical characteristics. Therefore, in Figure 16 and 17, the single error or time consuming at most time points is better than the average. It is because when calculating the average value, this abrupt characteristic is diluted. But from a holistic point of view, the performance of single optimization is still better than the other three methods.

Due to the randomness of re-planning, in the comparison and subsequent application of the algorithm, it is necessary to consider both its statistical characteristics and its own random characteristics in order to better use the algorithm in this paper.

VIII. CONCLUSION

Based on the MI criterion, this paper jointly optimizes the spatial position and radiated power of the airborne MIMO radar. Radar detection efficiency has been improved.

By constructing the MIMO radar cooperative detection model of the aviation cluster, the effects of radar position and radiation strategy on detection are derived. The MI of the radar transmitted and received signals and the MI of the echoes at neighboring moments are derived, and the relationship between the radar position and radiated power and these two information volumes is constructed. Maximizing the amount of MI between the transmitted and received signals can obtain more information about the detected target. Minimizing the amount of MI at adjacent moments can improve the independence of detection and the quality of the detection signal. In view of the shortcomings of the ABC method, it is improved from the search method of algorithm level and algorithm adaptability. Using the IABC algorithm combined with time-sharing optimization strategy, combined with aircraft feasibility and energy constraints, the above two objective functions are optimized to achieve joint optimization of MIMO radar spatial position and radiated power. Through simulation comparison, it is shown that the algorithm of this paper is superior to the mainstream MIMO radar resource allocation algorithm and other improved ABC algorithm.

ACKNOWLEDGMENT

The authors would like to thank the anonymous reviewers for their valuable and constructive comments.

REFERENCES

[1] A. Haimovich, R. Blum, and L. Cimini, "MIMO radar with widely separated antennas," *IEEE Signal Process. Mag.*, vol. 25, no. 1, pp. 116–129, 2008.

[2] Y. Chen, B. Weng, and J. Liu, "A novel photonic-based MIMO radar architecture with all channels sharing a single transceiver," *IEEE Access*, vol. 7, pp. 165093–165102, 2019.

[3] X. Hu, C. Feng, Y. Wang, and Y. Guo, "Adaptive waveform optimization for MIMO radar imaging based on sparse recovery," *IEEE Trans. Geosci. Remote Sens.*, vol. 58, no. 4, pp. 2898–2914, Apr. 2020.

[4] S. Fortunati, L. Sanguinetti, F. Gini, M. S. Greco, and B. Himed, "Massive MIMO radar for target detection," *IEEE Trans. Signal Process.*, vol. 68, pp. 859–871, 2020.

[5] B. Xu and Y. Zhao, "Transmit beamspace-based unitary parallel factor method for DOD and DOA estimation in bistatic MIMO radar," *IEEE Access*, vol. 6, pp. 65573–65581, 2018.

[6] J. Xiong, W.-Q. Wang, and K. Gao, "FDA-MIMO radar range–angle estimation: CRLB, MSE, and resolution analysis," *IEEE Trans. Aerosp. Electron. Syst.*, vol. 54, no. 1, pp. 284–294, Feb. 2018.

[7] K. Alhujaili, V. Monga, and M. Rangaswamy, "Transmit MIMO radar beampattern design via optimization on the complex circle manifold," *IEEE Trans. Signal Process.*, vol. 67, no. 13, pp. 3561–3575, Jul. 2019.
[8] Y. Liu, X. Xu, and G. Xu, "MIMO radar calibration and imagery for near-field scattering diagnosis," *IEEE Trans. Aerosp. Electron. Syst.*, vol. 54, no. 1, pp. 442–452, Feb. 2018.
[9] W. Feng, Y. Guo, X. He, H. Liu, and J. Gong, "Jointly iterative adaptive approach based space time adaptive processing using MIMO radar," *IEEE Access*, vol. 6, pp. 26605–26616, 2018.
[10] B. Tang, J. Tuck, and P. Stoica, "Polyphase waveform design for MIMO radar space time adaptive processing," *Signal Process.*, 2020.
[11] H. Godrich, A. P. Petropulu, and H. V. Poor, "Power allocation strategies for target localization in distributed multiple-radar architectures," *IEEE Trans. Signal Process.*, vol. 59, no. 7, pp. 3226–3240, Jul. 2011.
[12] Y. Lu, C. Han, Z. He, S. Liu, and Y. Wang, "Adaptive JSPA in distributed colocated MIMO radar network for multiple targets tracking," *IET Radar, Sonar Navigat.*, vol. 13, no. 3, pp. 410–419, Mar. 2019.
[13] Z. Li, J. Xie, and H. Zhang, "Joint power and time width allocation in collocated MIMO radar for multi-target tracking," *IET Radar, Sonar Navigat.*, vol. 14, no. 5, pp. 686–693, May 2020.
[14] N. Garcia, A. M. Haimovich, M. Coulon, and M. Lops, "Resource allocation in MIMO radar with multiple targets for non-coherent localization," *IEEE Trans. Signal Process.*, vol. 62, no. 10, pp. 2656–2666, May 2014.
[15] H. Zhang, J. Xie, J. Shi, Z. Zhang, and X. Fu, "Sensor scheduling and resource allocation in distributed MIMO radar for joint target tracking and detection," *IEEE Access*, vol. 7, pp. 62387–62400, 2019.
[16] J. Yan, H. Liu, W. Pu, S. Zhou, Z. Liu, and Z. Bao, "Joint beam selection and power allocation for multiple target tracking in netted colocated MIMO radar system," *IEEE Trans. Signal Process.*, vol. 64, no. 24, pp. 6417–6427, Dec. 2016.
[17] W. Yi, Y. Yuan, R. Hoseinnezhad, and L. Kong, "Resource scheduling for distributed multi-target tracking in netted colocated MIMO radar systems," *IEEE Trans. Signal Process.*, vol. 68, pp. 1602–1617, 2020.
[18] B. Ma, H. Chen, B. Sun, and H. Xiao, "A joint scheme of antenna selection and power allocation for localization in MIMO radar sensor networks," *IEEE Commun. Lett.*, vol. 18, no. 12, pp. 2225–2228, Dec. 2014.
[19] J. Yan, B. Jiu, H. Liu, B. Chen, and Z. Bao, "Prior knowledge-based simultaneous multibeam power allocation algorithm for cognitive multiple targets tracking in clutter," *IEEE Trans. Signal Process.*, vol. 63, no. 2, pp. 512–527, Jan. 2015.
[20] Y. Ma, S. Chen, C. Xing, X. Bu, and L. Hanzo, "Decomposition optimization algorithms for distributed radar systems," *IEEE Trans. Signal Process.*, vol. 64, no. 24, pp. 6443–6458, Dec. 2016.
[21] A. Deligiannis, A. Panoui, S. Lambotharan, and J. A. Chambers, "Game-theoretic power allocation and the Nash equilibrium analysis for a multistatic MIMO radar network," *IEEE Trans. Signal Process.*, vol. 65, no. 24, pp. 6397–6408, Dec. 2017.
[22] A. Deligiannis, S. Lambotharan, and J. A. Chambers, "Game theoretic analysis for MIMO radars with multiple targets," *IEEE Trans. Aerosp. Electron. Syst.*, vol. 52, no. 6, pp. 2760–2774, Dec. 2016.
[23] X. Zhang, H. Ma, J. Wang, S. Zhou, and H. Liu, "Game theory design for deceptive jamming suppression in polarization MIMO radar," *IEEE Access*, vol. 7, pp. 114191–114202, 2019.
[24] J. Yan, W. Pu, H. Liu, B. Jiu, and Z. Bao, "Robust chance constrained power allocation scheme for multiple target localization in colocated MIMO radar system," *IEEE Trans. Signal Process.*, vol. 66, no. 15, pp. 3946–3957, Aug. 2018.
[25] H. Zhang, W. Liu, J. Xie, Z. Zhang, and W. Lu, "Joint subarray selection and power allocation for cognitive target tracking in large-scale MIMO radar networks," *IEEE Syst. J.*, vol. 14, no. 2, pp. 2569–2580, Jun. 2020.
[26] H. Zheng, B. Jiu, and H. Liu, "Joint optimization of transmit waveform and receive filter for target detection in MIMO radar," *IEEE Access*, vol. 7, pp. 184923–184939, 2019.
[27] H. Chen, S. Ta, and B. Sun, "Cooperative game approach to power allocation for target tracking in distributed MIMO radar sensor networks," *IEEE Sensors J.*, vol. 15, no. 10, pp. 5423–5432, Oct. 2015.
[28] B. Sun, H. Wang, X. Wei, H. Chen, and X. Li, "Power allocation for range-only localisation in distributed multiple-input multiple-output radar networks–A cooperative game approach," *IET Radar, Sonar Navigat.*, vol. 8, no. 7, pp. 708–718, Aug. 2014.
[29] Y. Yu, S. Sun, R. N. Madan, and A. Petropulu, "Power allocation and waveform design for the compressive sensing based MIMO radar," *IEEE Trans. Aerosp. Electron. Syst.*, vol. 50, no. 2, pp. 898–909, Apr. 2014.
[30] A. Ajorloo, A. Amini, and M. H. Bastani, "A compressive sensing-based colocated MIMO radar power allocation and waveform design," *IEEE Sensors J.*, vol. 18, no. 22, pp. 9420–9429, Nov. 2018.
[31] C. Shi, F. Wang, M. Sellathurai, and J. Zhou, "Low probability of intercept-based distributed MIMO radar waveform design against barrage jamming in signal-dependent clutter and coloured noise," *IET Signal Process.*, vol. 13, no. 4, pp. 415–423, Jun. 2019.
[32] M. J. Ghoreishian, S. M. Hosseini Andargoli, and F. Parvari, "Power allocation in MIMO radars based on LPI optimisation and detection performance fulfilment," *IET Radar, Sonar Navigat.*, vol. 14, no. 6, pp. 822–832, Jun. 2020.
[33] B. Tang, J. Tang, and Y. Peng, "MIMO radar waveform design in colored noise based on information theory," *IEEE Trans. Signal Process.*, vol. 58, no. 9, pp. 4684–4697, Sep. 2010.
[34] J. Wang, X.-D. Liang, L.-Y. Chen, L.-N. Wang, and K. Li, "First demonstration of joint wireless communication and high-resolution SAR imaging using airborne MIMO radar system," *IEEE Trans. Geosci. Remote Sens.*, vol. 57, no. 9, pp. 6619–6632, Sep. 2019.
[35] C. Wen, J. Peng, Y. Zhou, and J. Wu, "Enhanced three-dimensional joint domain localized STAP for airborne FDA-MIMO radar under dense false-target jamming scenario," *IEEE Sensors J.*, vol. 18, no. 10, pp. 4154–4166, May 2018.
[36] J. Wang, S. Jiang, J. He, and Z. Liu, "Adaptive detectors with diagonal loading for airborne multi-input multi-output radar," *IET Radar Sonar Navigat.*, vol. 3, no. 5, pp. 493–501, 2009.
[37] R. S. Raghavan, "Coherent airborne MIMO detection of multiscatter targets," *IEEE Trans. Aerosp. Electron. Syst.*, vol. 54, no. 2, pp. 978–991, Apr. 2018.
[38] W. Gao, H. Sheng, J. Wang, and S. Wang, "Artificial bee colony algorithm based on novel mechanism for fuzzy portfolio selection," *IEEE Trans. Fuzzy Syst.*, vol. 27, no. 5, pp. 966–978, May 2019.
[39] J.-Q. Li, M.-X. Song, L. Wang, P.-Y. Duan, Y.-Y. Han, H.-Y. Sang, and Q.-K. Pan, "Hybrid artificial bee colony algorithm for a parallel batching distributed flow-shop problem with deteriorating jobs," *IEEE Trans. Cybern.*, vol. 50, no. 6, pp. 2425–2439, Jun. 2020.
[40] F. Dahan, H. Mathkour, and M. Arafah, "Two-step artificial bee colony algorithm enhancement for QoS-aware Web service selection problem," *IEEE Access*, vol. 7, pp. 21787–21794, 2019.
[41] S. Zhou, X. Xu, Z. Xu, W. Chang, and Y. Xiao, "Fractional-order modeling and fuzzy clustering of improved artificial bee colony algorithms," *IEEE Trans. Ind. Informat.*, vol. 15, no. 11, pp. 5988–5998, Nov. 2019.

XIANGYU FAN was born in 1991. He received the bachelor's degree in radar engineering and the master's degree in information and communication engineering from the School of Aeronautics and Astronautics Engineering, Air Force Engineering University, in 2014 and 2016, respectively, where he is currently pursuing the Ph.D. degree. He has published more than ten journal articles as the major author, among them, eight articles were retrieved by SCI/EI. He has finished four projects during his master's degree. He is involved in national key projects. His research interests include signal processing, and electronic countermeasure theory and technology.

PENG BAI was born in 1961. He received the bachelor's degree in radar engineering from the School of Aeronautics and Astronautics Engineering, Air Force Engineering University, in 1983, and the master's degree in information and communication engineering from Northwestern Polytechnical University, in 1989. He is currently a Professor with the School of Equipment Development and Application Research Center, Air Force Engineering University. He has published more than 120 journal articles as the major author, among them, 30 articles were retrieved by SCI and 37 by EI. He is the Chief Expert and the Main Person Responsible for a number of national key scientific research projects. His current research interests include advanced electronic science and technology in the future, and science and technology of network information system in the future. He received the National Science and Technology Progress Award for several times. He was commended by the president of China.

HONGWEI WANG was born in 1974. He is currently an Associate Professor with the School of Aeronautics and Astronautics Engineering, Air Force Engineering University. He studied video compression coding and artificial intelligence neural networks in the past; however, his current research interests include electromagnetic theory and now mainly about signal separation and recognition, and characters of controlling noise. He received a lot of prizes of the Military Science and Technology Progress Award.

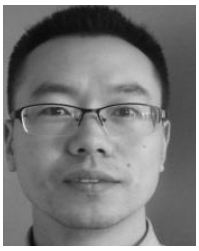

JIAQIANG ZHANG was born in 1984. He received the master's degree in weapon system and application engineering and the Ph.D. degree in armament science and technology from the School of Aeronautics and Astronautics Engineering, Air Force Engineering University, in 2009 and 2012, respectively. He is currently a Lecturer with the Air Traffic Control and Navigation College, Air Force Engineering University. He has published more than 20 journal articles and finished more than ten projects. His research interests include aviation cluster technology and airspace management intelligence.

HUANYU LI was born in 1984. He received the master's degree in computer application and the Ph.D. degree in information warfare from the School of Aeronautics and Astronautics Engineering, Air Force Engineering University, in 2009 and 2012, respectively. He is currently a Lecturer with the Air Traffic Control and Navigation College, Air Force Engineering University. He has published more than ten journal articles and finished more than ten projects. His research interests include machine learning and pattern recognition.